Band-Moment Analysis of Imaging-Spectrometer Data

Donald C. Rundquist
Center for Advanced Land Management Information Technologies, Conservation and Survey Division, Institute of Agriculture and Natural Resources, University of Nebraska-Lincoln, Lincoln, NE 68588–0517
Liping Di
Department of Geography, University of Nebraska-Lincoln, Lincoln, NE 68588–0135

ABSTRACT: Modern sensor systems high in spectral resolution, such as the Airborne Imaging Spectrometer (AIS), are challenging from an image-processing standpoint because direct classification of datasets with 100 or more spectral channels is virtually impossible. Thus, it is necessary to conduct pre-classification manipulations and transformations both to reduce the amount of data to be classified and to extract pertinent information from the original dataset. Band-moment analysis is a simple, computationally efficient, and productive alternative to principal-components analysis (PCA), a technique commonly used for data reduction. Results from moment analysis of AIS-1 data for western Nebraska are compared to those derived from PCA. Although additional work is warranted, especially concerning the physical meaning of individual moments, several advantages of moment analysis are documented including computational efficiency, reduction of sensor noise, and an overall image quality which is at least as good as a first-principal-component image.

INTRODUCTION

FUNDAMENTAL TO REMOTE SENSING is the concept of multispectral information providing quantitative signatures for terrain features and land cover. Multispectral classification techniques are commonly employed for statistical identification of these signatures and for sorting individual pixels into themes that can be mapped (e.g., Jensen, 1986).

Classification algorithms for remotely sensed data are commonly based on image-feature extraction. In the case of multispectral images, the simplest features are the pixel-brightness values or digital numbers (DN) in each spectral channel sampled by the sensor. These features are not, however, necessarily the best to use for accurate classification because the signal can be degraded by factors such as atmospheric attenuation and topographic relief (Robinove, 1982). Another problem is the fact that per-channel DNs of a multispectral image are often highly correlated, and thus are redundant in terms of information content. Furthermore, the computational time needed for classification increases exponentially with an increase in the number of variables (channels) analyzed. In some instances, the direct classification of an original multispectral image is, for all practical purposes, impossible when the number of bands is very large. Thus, various pre-classification manipulations and transformations have been developed both to reduce the amount of data to be classified and to extract the critical features from the original dataset prior to actual image classification.

Principal-components analysis (PCA), one of the most common pre-classification processing techniques for feature extraction, serves to significantly reduce data dimensionality; i.e., it mitigates spectral redundancy (Siegal and Gillespie, 1980). Resultant principal-component images are uncorrelated and are ordered by decreasing amounts of DN variance. Therefore, the overall visual quality of component images decreases from first to successive components. Because the DN variance is diminished markedly from the first to second and subsequent components, most of the information present in the original multispectral dataset is contained in the first-component image (Moik, 1980). Thus, derivation of principal-component images often provides advantages including (1) compressing data-set variance into one or two images, (2) relegating noise to second or lower-component images, and (3) occasionally highlighting spectral differences in surface materials which may not be apparent in the original individual channels (Sabins, 1987). When one is presented with a very large number of spectral channels to process, PCA can also be helpful in developing features for input to conventional classification algorithms.

THE AIRBORNE IMAGING SPECTROMETER (AIS)

The imaging spectrometer program, initiated with NASA funding in 1981 at the Jet Propulsion Laboratory (JPL), has developed high-spectral-resolution imaging sensors (NASA, 1987). The first system to evolve from this program was the Airborne Imaging Spectrometer-1 (AIS-1).

"AIS was built originally as an engineering test bed for two-dimensional infrared detector arrays operating in the 0.8 to 2.5 micrometre (μm) region" (Vane, 1987). AIS-1 data were first acquired in 1983, and since that time, improved airborne systems for imaging spectroscopy have provided scientists with "a powerful new class of data for identifying and assessing the characteristics of surface materials" (Vane, 1987).

The AIS-1 made use of a 32 by 32 element mercury-cadmium-telluride (HgCdTe) detector array to acquire simultaneously 128 images in very narrow (9.3 nm) spectral bands (Vane and Goetz, 1985). Data collection in these 128 channels is facilitated by a grating which tilts through four separate positions as the sensor platform moves forward one ground instantaneous field of view (IFOV). The AIS had an IFOV of 1.9 mrad and a nominal ground pixel size of 8 by 8 metres for a typical operating altitude of 4200 metres (Goetz *et al.*, 1985). Thus, a resulting dataset consisted of 128 arrays, each 32 pixels wide for a given flight corridor (n scan lines). The DN dynamic range for each pixel and channel of raw AIS data is 0 to 4095, so it requires 12 bits for storage (Jet Propulsion Laboratory, 1985).

When AIS-1 data were first provided to investigators by JPL, it became clear that new techniques and concepts would be needed for data characterization and analysis. Even casual perusal of the written reports on initial research serves to support this contention. Many varied methods and approaches were tested, including Walsh-Hadamard transformations (Wickland, 1985), "cross-band" correlation (Vanderbilt, 1985), principal components (Smith and Adams, 1985; Bell and Evans, 1985; Olson and Zhu, 1985; Hutsinpiller, 1988; Feldman and Taranik, 1988), "radiance ratios" (Vanderbilt, 1985; Gross and Klemas, 1985), band ratios

PHOTOGRAMMETRIC ENGINEERING AND REMOTE SENSING,
Vol. 55, No. 2, February 1989, pp, 203–208.
0099-1112/89/5502–203$02.25/0

(Feldman and Taranik, 1988), discriminant analysis (Blad *et al.*, 1985; Olson and Zhu, 1985), cluster analysis (Samson, 1985), Fourier transforms (Kruse *et al.*, 1985; Hlavka, 1986; Swanberg and Matson, 1987; Price and Westman, 1987), log residuals (Lyon and Lanz, 1985; Cocks and Green, 1986; Lyon, 1987; Hutsinpiller, 1988), "hull" quotients (Green and Craig, 1985; Clark, *et al.*, 1987), principal factor analysis (Murray *et al.*, 1986), "internal average relative reflectance" (Mackin *et al.*, 1987; Kruse, 1987), multiple regression (Peterson *et al.*, 1988), and numerous others. Like many of these earlier works which attempt to either shed light on the nature of imaging-spectrometer data or to expedite data handling of 128 channels by applying a variety of techniques, our work is clearly exploratory.

Some investigators have taken an image-classification approach with AIS data (e.g., Feldman *et al.*, 1985; Masuoka, 1985; Ustin *et al.*, 1986; Herrmann *et al.*, 1988). However, because the AIS produces 128 separate channels of spectral information, image classification has been found to be a significant computational and logistical problem. General purpose software for image classification (e.g., ELAS, LAS, ERDAS) usually is limited to processing between eight and 30 channels of spectral data. Even if software were available to accommodate 100 or more bands, the machine time necessary for the classification would make the processing infeasible or, at least, uneconomical.

In the case of the AIS, it is necessary somehow to reduce the dimensionality of the original data. PCA allows one to perform a pre-classification data compression. Even with PCA, though, much computational time is required both for the calculation of the covariance matrix and for matrix multiplication. Fast PCA algorithms seem not to exist. This fact is underscored when processing AIS data to compute a 128 by 128 covariance matrix. Note, too, that every component requires 128 real multiplications. In addition, we have found that, when original images contain sensor noise (e.g., "striping"), some component images will display that noise very prominently. Masuoka (1985) and Hlavka (1986) documented several types of noise in raw AIS data, but the latter author focused on pronounced striping in both the vertical and horizontal directions.

Objectives

In this paper, we introduce what we believe to be a relatively simple and efficient new procedure, "band-moment analysis," for use in reduction of AIS data. Our goal is to introduce a computationally efficient technique for analyzing high-spectral-resolution data which yields images that are at least as good in visual quality as those produced by means of principal-component analysis. Procedures outlined in this paper should be equally applicable both to AIS-1 and to follow-on systems including AIS-2, AVIRIS, and HIRIS (NASA, 1987).

BAND-MOMENT ANALYSIS

The digital numbers (or DN) for each band of a multispectral image represent the reflection or emission of electromagnetic energy in a specified wavelength range. A plot of pixel DNs versus wavelength represents the change in reflectance or emittance of a pixel with change in wavelength (Figure 1). Such a set of measurements constitutes a spectral-response pattern or "spectral signature" for ground objects or surfaces (Campbell, 1987). In the case of the AIS, the spectral-response pattern is very detailed, being composed of reference points stemming from 128 narrow, contiguous bands (Figure 1). Classification algorithms for multispectral image analysis are designed to identify and group pixels having similar spectral signatures. If a signature (or spectral curve such as Figure 1) can be described quantitatively by a set of features, then the measure is said to summarize those features of the curve by means of mathematical notation. This "shorthand," which may consist of only a few quantitative features, is especially important when analyzing 100 or more bands of sensor data.

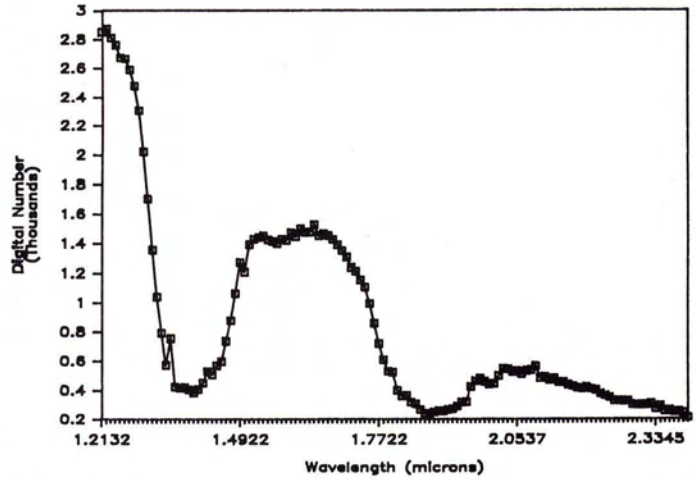

FIG. 1. Example of a spectral-response profile for a pixel containing a stand of cattails. Data were acquired by the Airborne Imaging Spectrometer-1 on 16 June 1985 in western Nebraska.

"Moments," which exist in statistics, are quantities that describe the distribution of variables, i.e., the character of a distribution curve (Edwards, 1964; Cole and King, 1968; King, 1969). Moment measures include the mean, standard deviation, skewness, and kurtosis, which are generally referred to as the first, second, third, and fourth statistical moments (e.g., Cole and King, 1968). However, it is possible to derive other moments mathematically. Using AIS channels as variables, we introduce "band-moment analysis," and derive a series of eight moments.

Suppose the wavelength (λ) of an electromagnetic wave is an independent variable. The reflectance from a ground object $f(\lambda)$ is a continuous function of λ. We define the moment of order p by the relation

$$Mp = \int_0^{\infty} \lambda^p f(\lambda) d\lambda \qquad p = 0, 1, 2. . . \tag{1}$$

According to the "uniqueness" theorem (Papoulis, 1965), if $f(\lambda)$ is piecewise continuous and has nonzero values only in a finite part of the axis, then moments of all orders exist and the moment sequence Mp is uniquely determined by $f(\lambda)$ and, conversely, Mp uniquely determines $f(\lambda)$. This theorem expresses the fact that the moments can represent $f(\lambda)$.

The central moments can be expressed (similar to Skopp (1987)) as

$$\mu_p = \int_0^{\infty} (\lambda - \bar{\lambda})^p f(\lambda) d\lambda \tag{2}$$

where $\bar{\lambda} = \frac{M_1}{M_0}$.

For the particular and discrete case of AIS data, we define the band moments as follows:

$$Mp = \frac{1}{128} \sum_{i=1}^{128} i^{p*} f(i) \qquad p = 0, 1, 2. . . . \tag{3}$$

where $f(i)$ is the pixel DN in band i of AIS data.

The central band moments can be expressed as

$$\mu_p = \frac{1}{128} \sum_{i=1}^{128} (i - \bar{i})^p f(i) \qquad p = 0, 1, 2, \ldots \tag{4}$$

where $\bar{i} = \frac{M_1}{M_0}$.

The first central band moment always is equal to zero because

$$\mu_1 = \frac{1}{128} \sum_{i=1}^{128} (i - \bar{i}) f(i) = M_1 - \frac{M_1}{M_0} * M_0 = 0$$

For ease of understanding, we consider the DN in band i as the frequency (or weight) of this channel. Then $\bar{i}$ suggests that the mean band of a particular pixel is weighted by DN. We refer to $\bar{i}$ as the "band mean." Comparison of μ_2 with the variance shows them to be the same quantity, so μ_2 can be denoted as band variance. For $q = 3$, the central band moment represents the assymmetry of the density-band curve. For $p = 4$, the central band moment indicates the degree of spread in the curve, particularly emphasizing values apart from the band mean.

In addition, we introduce two band ratios to the density band curve analysis. The first is called "band skewness":

$$\gamma_1 = \mu_3/\mu_2^{3/2} \tag{5}$$

and second is "band kurtosis":

$$\gamma_2 = \mu_4/\mu_2^2 - 3 \tag{6}$$

Positive values of skewness indicate that the pixel has high DNs for the first several bands and low DNs for the last several bands (tailing to the right), while negative values depict the opposite (tailing to the left). Values of skewness and kurtosis near zero indicate a data distribution resembling a normal bell shape. Symmetrical curves will always have zero for the value of the third central band moment (or band skewness).

Up to this point, all formulae we have described place emphasis on two sides of the density-band curve. In order to emphasize channels near the band mean, another moment, a "band-concentrated moment," is introduced: i.e.,

$$\mu_{2c} = \frac{1}{128} \sum_{i=1}^{128} (i - |i - \bar{i}|)^2 f(i) \tag{7}$$

Thus, for every pixel of an AIS image, we calculate eight values: $\bar{i}$, M_0, μ_2, μ_3, μ_4, γ_1, γ_2, and μ_{2c}. While it is extremely difficult to describe all eight of these moments in non-quantitative terms, we refer to them as follows: (1) mean, (2) ordinary moment, (3) variance, (4) third central moment, (5) fourth central moment, (6) skewness, (7) kurtosis, and (8) band-concentrated moment. The result consists of a new eight-band image which has features derived from the original 128-band image; i.e., the eight "channels" of the new image retain the general statistical characteristics of the original 128-channel dataset. Because real numbers are calculated from the formulae, the DNs of the new image are compressed linearly to integers 0 to 255 for display and classification purposes. The calculation of μ is much easier than that of PCA and can be executed recursively.

IMPLEMENTATION

To evaluate the effectiveness of band-moment analysis, we selected an AIS dataset from a NASA C-130 flightline obtained in the western portion of the Nebraska Sand Hills (Figure 2) on 16 June 1985 (earlier work with AIS datasets in Nebraska is summarized in Blad *et al.* (1985), Samson (1985) Rundquist (1985), and Samson, (1988). The size of our study area was 300 by 32 pixels (see Figure 2 for geographic location). Figure 3 depicts

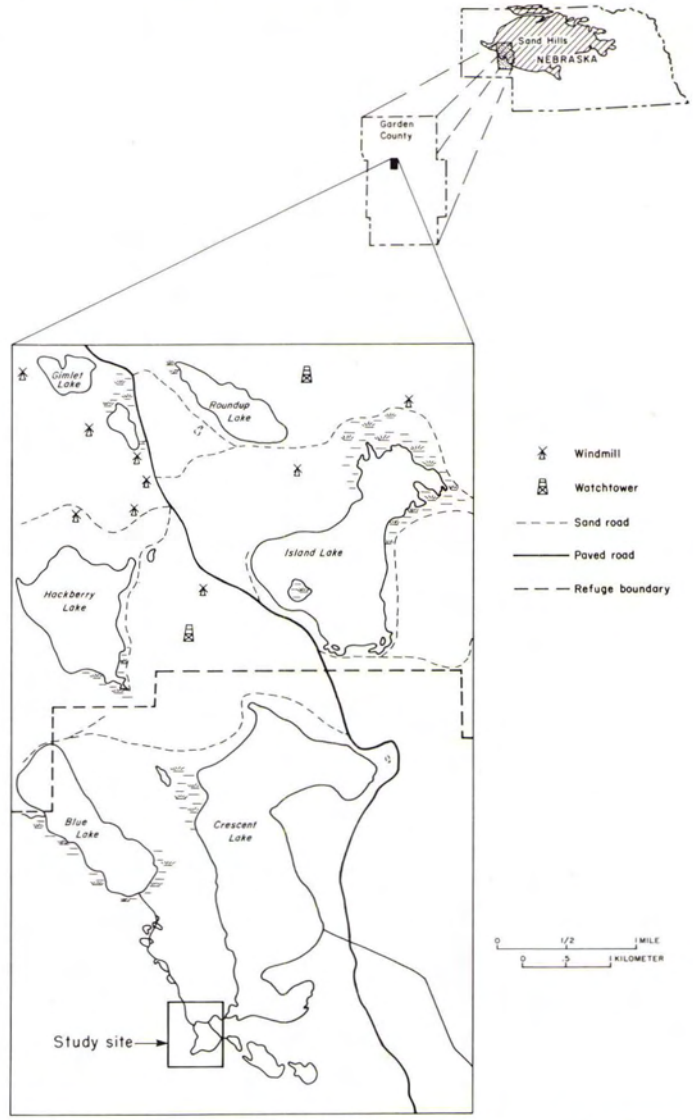

FIG. 2. The study site located within the Crescent Lake National Wildlife Refuge, Garden County, Nebraska.

only the first 16 bands (1.2132 to 1.3527 μm) of the AIS image. Figure 4 is a photographic enlargement of the study site taken from a conventional air photo of the Crescent Lake area. Notice in Figure 3 that sensor striping (both vertical and horizontal) is apparent in channels 9 to 16 with image quality severely degraded by sensor noise in bands 13 to 16. Such a problem was typical of AIS data acquired in 1984 and 1985 (Hlavka, 1986). It should also be pointed out that a strong atmospheric water-absorption band exists at 1.4 μm (and also at 1.9 μm) making remote sensing in this spectral region difficult (Goetz *et al.*, 1983). The imaged area shown for each channel is, of course, identical and, when examined in conjunction with the conventional air photo of the site (Figure 4), identification of a few landscape parameters is possible. For example, one can see some evidence of dune topography, a tiny lake, and a small stream channel. More detailed interpretation is difficult.

An eight-moment image of the study area was prepared from raw 12-bit (0 to 4095 DN) AIS data in order to assess its utility for both data reduction and image enhancement (Figure 5). During calculation from raw data, each resulting moment dataset was compressed linearly to eight bits (0 to 255 DN) to

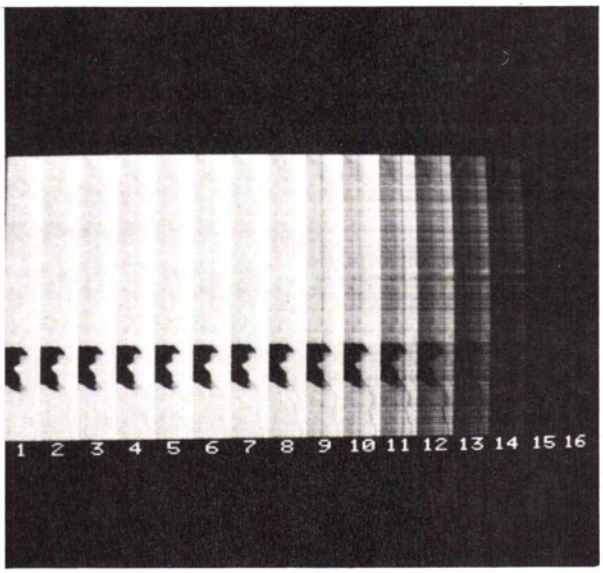

FIG. 3. AIS channels 1 to 16 for the study site. Each individual swath is 32 by 300 pixels. Also, because of mission parameters, note that north is at the bottom.

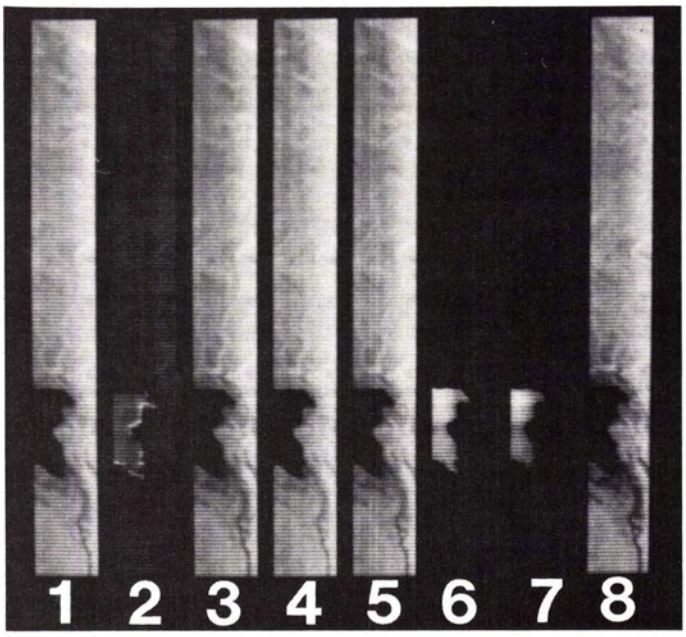

FIG. 5. Eight-moment AIS image of the study area. Note the improvement in image clarity over the raw data (Figure 3).

FIG. 4. Panchromatic air-photo enlargement of the study site. Date of photography is 4 November 1982, and north is at the bottom. For scale reference, refer to Figure 2.

allow image display. Note, first of all, that the sensor noise (striping) in the raw data (Figure 3) has been virtually eliminated in the moment images (Figure 5) due to the averaging which occurs in the moment calculation (see computations above). Secondly, the images for five of the eight moments are generally similar but, more importantly, they are also quite "crisp." The skewness and kurtosis images, while providing no information about the land surface (as displayed by means of a linear compression), are quite different from the other moments; in fact, surface water is characterized by very light tones in the moment-6 and -7 images. The image for the second moment, like the sixth and seventh moments, is also somewhat different and relatively poor. One final point which seems worthy of mention is the fact that the image for the eighth moment possesses an overall tonal quality that is subtly different from moments 1, 3, 4, and 5. The reason for this difference is not apparent to us.

To compare the visual quality of band-moment images with that of principal-component images, the first eight (PCA) components were also computed from raw 12-bit AIS data, and compressed linearly to eight bits for image display (Figure 6). Notice that the first component image is, as expected, quite crisp and clear, while the others (also as expected) are not nearly as good. Horizontal sensor striping dominates in component images 2 (worst), 4, and 3 while vertical striping seems to be equally pronounced in component images 6 and 7. Component images 8 and 5 possess both horizontal and vertical stripes. Masuoka (1985) noticed noise in components 2 and 4 after a PCA transformation of only the first 32 bands of October 1983 data acquired in West Virginia. Thus, it is apparent that PCA does not remove sensor striping as do moment procedures. With regard to information content, the first-component image is, according to the inherent qualities of PCA, quite useful and interpretable, but may be no better in overall clarity than the image of the first (or selected other) moments (compare Figures 5 and 6). Our concern is that very few AIS component images seem useful, although the component 3 image may be an exception (notice, especially, the detail in the area around the lake). On the other hand, five of the moment images provide (at least) good-quality images of the flight corridor. Importantly, we found that the computation time for PCA was roughly four times greater than that for moment analysis.

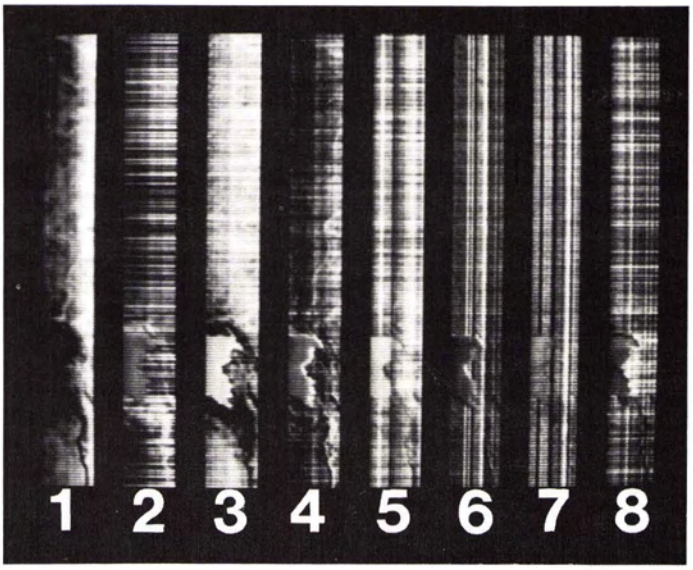

FIG. 6. First eight principal components for the study site.

CONCLUSION

We conclude that band-moment analysis is a useful technique for data reduction and enhancement of AIS data. It is much easier and more computationally efficient than principal-components analysis. In fact, the execution time on our minicomputer was over four times greater for PCA than for moment analysis. In addition, it appears that, like PCA, moment analysis allows the user to compress the salient characteristics of a multispectral dataset into a few displayable features. Our results also indicate that band-moment analysis not only removes scanning noise, which is not mitigated by PCA, but it also yields a larger number of crisp, potentially useful images than PCA. We are unable to provide comment regarding the capability of moment analysis in the area of highlighting spectral differences in surface materials which may not be apparent in the original dataset because we have not yet investigated the physical meaning of individual moments as applied to AIS information for our study site. At the very least, band-moment analysis provides images that are as good in quality as those produced by means of PCA, but the former is much more efficient from a computational standpoint.

In addition to examining the physical meaning of signatures on moment images, our future research will address a comparative multispectral classification of features computed by both moment analysis and PCA. Also, we are interested in transposing the concept of moment analysis to the temporal domain; i.e., it should be possible to compute moments from multitemporal image data.

ACKNOWLEGMENT

The authors sincerely appreciate the professionalism and constructive criticism of one anonymous reviewer who contributed significantly to the publication of this paper.

REFERENCES

Bell, R., and C. S. Evans, 1985. Comparison of AIS vs. TMS data collected over the Virginia piedmont. *Proceedings of the Airborne Imaging Spectrometer Data Analysis Workshop*, NASA JPL Publication 85-41, pp. 120–122.

Blad, B. L., *et al.*, 1985. Evaluation of AIS data for agronomic and rangeland vegetation: preliminary results for August 1984 flight over Nebraska Sandhills agricultural laboratory. *Proceedings of the Airborne Imaging Spectrometer Data Analysis Workshop*, NASA JPL Publication 85-41, pp. 68–70.

Campbell, J. B., 1987. *Introduction to Remote Sensing*. New York: Guilford Press.

Clark, R. N., *et al.*, 1987. Automatic continuum analysis of reflectance spectra. *Proceedings of the Third Airborne Imaging Spectrometer Data Analysis Workshop*, NASA JPL Publication 87-30, pp. 138–142.

Cocks, T. D., and A. A. Green, 1986. *Proceedings of the Second Airborne Imaging Spectrometer Data Analysis Workshop*, NASA JPL Publication 86-35, pp. 52–62.

Cole, J. P., and C. A. M. King, 1968. *Quantitative Geography*. London: John Wiley and Sons.

Edwards, A. L., 1964. *Expected Values of Discrete Random Variables and Elementary Statistics*. New York: John Wiley and Sons.

Feldman, S. C., and J. V. Taranik, 1988. Comparison of techniques for discriminating hydrothermal alteration minerals with Airborne Imaging Spectrometer data. *Rem. Sen. Env.*, 24:67–83.

Feldman, S. C., *et al.*, 1985. A first look at Airborne Imaging Spectrometer (AIS) data in an area of altered volcanic rocks and carbonate formations, Hot Creek Range, South Central Nevada. *Proceedings of the Airborne Imaging Spectrometer Data Analysis Workshop*, NASA JPL Publication 85-41, pp. 56–61.

Goetz, A. F. H., *et al.*, 1983. Remote sensing for exploration: an overview. *Econ. Geol.*, 78:573–590.

———, 1985. Imaging spectrometry for earth remote sensing. *Science*, 228:1147–1153.

Green, A. A., and M. D. Craig, 1985. Analysis of aircraft spectrometer data with logarithmic residuals. *Proceedings of the Airborne Imaging Spectrometer Data Analysis Workshop*, NASA JPL Publication 85-41, pp. 111–119.

Gross, M. F., and V. Klemas, 1985. Discrimination of coastal vegetation and biomass using AIS data. *Proceedings of the Airborne Imaging Spectrometer Data Analysis Workshop*, NASA JPL Publication 85-41, pp. 129–133.

Herrmann, K., *et al.*, 1988. Preliminary assessment of Airborne Imaging Spectrometer and Airborne Thematic Mapper data acquired for forest decline areas in the Federal Republic of Germany. *Rem. Sen. Env.*, 24:129–149.

Hlavka, C., 1986. Destriping AIS data using fourier filtering techniques. *Proceedings of the Second Airborne Imaging Spectrometer Data Analysis Workshop*, NASA JPL Publication 86-35, pp. 74–80.

Hutsinpiller, A., 1988. Discrimination of hydrothermal alteration mineral assemblages at Virginia City, Nevada, using the Airborne Imaging Spectrometer. *Rem. Sen Env.*, 24:53–66.

Jensen, J. R., 1986. *Introductory Digital Image Processing*. Englewood Cliffs, New Jersey: Prentice-Hall.

Jet Propulsion Laboratory, 1985. *Science Investigators Guide to AIS Data.*

King, L. J., 1969. *Statistical Analysis in Geography*. Englewood Cliffs, New Jersey: Prentice-Hall.

Kruse, F. A., 1987. Mapping hydrothermally altered rocks in the northern Grapevine Mountains, Nevada and California with the Airborne Imaging Spectrometer. *Proceedings of the Third Airborne Imaging Spectrometer Data Analysis Workshop*, NASA JPL Publication 87-30, pp. 148–165.

Kruse, F. A., *et al.*, 1985. Analytical techniques for extracting mineralogical information from multichannel imaging spectrometer data. *Proceedings of the Airborne Imaging Spectrometer Data Analysis Workshop*, NASA JPL Publication 85-41, p. 105.

Lyon, R. J. P., 1987. Evaluation of AIS-2 (1986) data over hydrothermally altered granitoid rocks of the Singatse Range (Yerington) Nevada and comparison with 1985 AIS-1 data. *Proceedings of the Third Airborne Imaging Spectrometer Data Analysis Workshop*, NASA JPL Publication 87-30, pp. 107–119.

Lyon, R. J. P., and K. Lanz, 1985. Field utilization and analysis of AIS 128-channel imagery using microcomputers: application to Yerington, NV field area. *Proceedings of the Airborne Imaging Spectrometer Data Analysis Workshop*, NASA JPL Publication 85-41, pp. 35–40.

Mackin, S., *et al.*, 1987. Preliminary results from an investigation of AIS-1 data over an area of epithermal alteration: Plateau, Northern Queensland, Australia. *Proceedings of the Third Airborne Imaging*

Spectrometer Data Analysis Workshop, NASA JPL Publication 87-30, pp. 120–131.

Masuoka, E., 1985. A preliminary investigation of systematic noise in data acquired with the Airborne Imaging Spectrometer. *Proceedings of the Airborne Imaging Spectrometer Data Analysis Workshop*, NASA JPL Publication 85-41, pp. 123–128.

Moik, J. G., 1980. *Digital Processing of Remotely Sensed Images*. NASA SP-431, Washington, D.C.

Murray, R., *et al.*, 1986. AIS spectra of desert shrub canopies. *Proceedings of the Second Airborne Imaging Spectrometer Data Analysis Workshop*, NASA JPL Publication 86-35, pp. 187–193.

NASA, 1987. High-resolution imaging spectrometer: science opportunities for the 1990's. *Earth Observing System*, Vol. IIc, pp. 1–74.

Olson, C. E., Jr., and Z. Zhu, 1985. Forest species identification with high spectral resolution data. *Proceedings of the Airborne Imaging Spectrometer Data Analysis Workshop*, NASA JPL Publication 85-41, pp. 152–157.

Papoulis, A., 1965. *Probability, Random Variables, and Stochastic Process*. New York: McGraw-Hill.

Peterson, D. L., *et al.*, 1988. Remote sensing of forest canopy and leaf biochemical contents. *Rem. Sen. Env.*, 24:85–108.

Price, C. V., and W. E. Westman, 1987. Toward detecting California shrubland canopy chemistry with AIS data. *Proceedings of the Third Airborne Imaging Spectrometer Data Analysis Workshop*, NASA JPL Publication 87-30, pp. 91–99.

Robinove, C. J., 1982. Computation of physical values from Landsat digital data. *Photogrammetric Engineering and Remote Sensing*, 48(5):781–784.

Rundquist, D. C., 1985. Preliminary evaluation of AIS spectra along a topographic/moisture gradient in the Nebraska Sandhills. *Proceedings of the Airborne Imaging Spectrometer Data Analysis Workshop*, NASA JPL Publication 85-41, pp. 74–78.

Sabins, F. F., Jr., 1987. *Remote Sensing: Principles and Interpretation*. New York: W. H. Freeman and Co.

Samson, S. A., 1985. The use of AIS data for identifying and mapping calcareous soils in western Nebraska. Proceedings of the Airborne Imaging Spectrometer Data Analysis Workshop, NASA JPL Publication 85-41, pp. 79–83.

———, 1988. *The Use of High Spectral Resolution Imaging Spectrometry in the Delineation and Identification of Selected Soil Properties in the Western Sandhills of Nebraska*. Ph.D. dissertation, Department of Agronomy, University of Nebraska-Lincoln.

Siegel, B. S., and A. R. Gillespie (Eds.), 1980. *Remote Sensing in geology*. New York: John Wiley and Sons.

Skopp, J. M., 1987. Physical concepts of soils. Unpublished course notes, Department of Agronomy, University of Nebraska-Lincoln.

Smith, M. O., and J. B. Adams, 1985. Interpretation of AIS images of Cuprite, Nevada using constraints of spectral mixtures. *Proceedings of the Airborne Imaging Spectrometer Data Analysis Workshop*, NASA JPL Publication 85-41, pp. 62–67.

Swanberg, N. A., and P. A. Matson, 1987. The use of Airborne Imaging Spectrometer data to determine experimentally induced variation in coniferous canopy chemistry. *Proceedings of the Third Airborne Imaging Spectrometer Data Analysis Workshop*, NASA JPL Publication 87-30, pp. 70–74.

Ustin, S. L., 1986. Patterns of vegetation in Owens Valley, California. *Proceedings of the Second Airborne Imaging Spectrometer Data Analysis Workshop*, NASA JPL Publication 86-35, pp. 180–186.

Vanderbilt, V. C., 1985. Urban, forest, and agricultural AIS data: fine spectral structure. *Proceedings of the Airborne Imaging Spectrometer Data Analysis Workshop*, NASA JPL Publication 85-41, pp. 158–164.

Vane, G., 1987. Introduction to the proceedings of the Third Airborne Imaging Spectrometer (AIS) data analysis workshop. *Proceedings of the Third Airborne Imaging Spectrometer Data Analysis Workshop*, NASA JPL Publication 87-30, pp. 1–7.

Vane, G., and A. F. H. Goetz, 1985. Introduction to the proceedings of the Airborne Imaging Spectrometer (AIS) data analysis workshop. *Proceedings of the Airborne Imaging Spectrometer Data Analysis Workshop*, NASA JPL Publication 85-41, pp. 1–11.

Wickland, D. E., 1985. AIS spectra for stressed and unstressed plant communities in the Carolina slate belt. *Proceedings of the Airborne Imaging Spectrometer Data Analysis Workshop*, NASA JPL Publication 85-41, pp. 46–50.

(Received 21 June 1988; revised and accepted 25 October 1988)